

in "Nonlinear Conservation Laws and Applications"  
(A. Bressan, G.-Q. Chen, M. Lewicka and D. Wang, eds),  
IMA Volumes in Mathematics and its Applications #153,  
Springer NY, (2011), pp. 101-122.

SELECTED TOPICS IN APPROXIMATE SOLUTIONS  
OF NONLINEAR CONSERVATION LAWS.  
HIGH-RESOLUTION CENTRAL SCHEMES

EITAN TADMOR\*

**Central schemes** offer a simple and versatile approach for computing approximate solutions of non-linear systems of hyperbolic conservation laws and related PDEs. The solution of such problems often involves the spontaneous evolution of steep gradients. The multiscale aspect of these gradients poses a main computational challenge for their numerical solution. Central schemes utilize a minimal amount of information on the propagation speeds associated with the problems, in order to accurately detect these steep gradients. This information is then coupled with high-order, non-oscillatory reconstruction of the approximate solution in ‘the direction of smoothness’: that is, information of smoothness does not cross regions of steep gradients. The use of central stencils enables us to realize the reconstructed solutions through simple quadratures. In this manner, central schemes avoid the intricate and time-consuming details of the eigen-structure of the underlying PDEs, and in particular, the use of (approximate) Riemann solvers, dimensional splitting, etc. The resulting family of central schemes offers relatively simple, “black-box” solvers for a wide variety of problems governed by multi-dimensional systems of non-linear hyperbolic conservation laws and related convection-diffusion problems.

We highlight several features of this new class of central schemes. **Scalar equations.** Both the second- and third-order schemes were shown to have variation bounds, which in turn yield convergence with precise error estimates, as well as entropy and (multidimensional)  $L^\infty$ -stability estimates. **Systems of equations.** Extension to systems is carried out by *component-wise* application of the scalar framework. It is in this context that our central schemes offer a remarkable advantage over the corresponding upwind framework. **Multidimensional problems.** Since we bypass the need for (approximate) Riemann solvers, multidimensional problems are solved *without* dimensional splitting. In fact, the class of central schemes is utilized for a variety of nonlinear transport equations. A partial list of more than 120 references can be found in **CentPack**, [4]. CentPack is a collection of freely distributed C++ routines that implement a number of high-order, non-oscillatory central schemes for hyperbolic systems of conservation laws in one- and two-space dimensions,  $\mathbf{u}_t + \mathbf{f}(\mathbf{u})_x + \mathbf{g}(\mathbf{u})_y = 0$ .

---

\*Department of Mathematics, Institute for Physical Science and Technology and Center of Scientific Computation and Mathematical Modeling (CSCAMM), University of Maryland, College Park, MD 20742, USA ([tadmor@cscamm.umd.edu](mailto:tadmor@cscamm.umd.edu); <http://www.cscamm.umd.edu/~tadmor>). Research was supported in part by NSF grants FRG07-57227, DMS10-08397, and ONR grant N000140910385.

The numerical algorithm for the implementation of central schemes consists of two main steps: (i) a non-oscillatory piecewise polynomial reconstruction of point values from their cell averages; followed by (ii) time evolution of the reconstructed polynomial, which is governed by the flux functions  $\mathbf{f}(\cdot)$  and  $\mathbf{g}(\cdot)$ .

The efficiency and versatility of central schemes resides, mainly, in their simplicity: they eliminate the need for Riemann solvers and avoid dimensional splitting, yielding a generic formulation valid for any hyperbolic system that can be written in the above form. Only information specific to the model and problem to be solved needs to be provided; namely, a description of the flux functions,  $\mathbf{f}(\mathbf{u})$  and  $\mathbf{g}(\mathbf{u})$ , the maximal propagation speed, and the appropriate initial and boundary conditions.

**1. Introduction.** In recent years, central schemes for approximating solutions of hyperbolic conservation laws, received a considerable amount of renewed attention. A family of high-resolution, non-oscillatory, *central* schemes, was developed to handle such problems. Compared with the 'classical' *upwind* schemes, these *central* schemes were shown to be both simple and stable for a large variety of problems ranging from one-dimensional scalar problems to multi-dimensional systems of conservation laws. They were successfully implemented for a variety of other related problems, such as, e.g., the incompressible Euler equations [30], [24], [22], [23], the magneto-hydrodynamics equations [5], viscoelastic flows—[22] hyperbolic systems with relaxation source terms [6], [43], [1] non-linear optics, [10], traffic flow [26], and a host of other applications listed on the “central-station” site, <http://www.cscamm.umd.edu/centpack/publications/>.

The family of high-order *central* schemes we deal with, can be viewed as a direct extension to the first-order, Lax-Friedrichs (LxF) scheme [12], which on one hand is robust and stable, but on the other hand suffers from excessive dissipation. To address this problematic property of the LxF scheme, a Godunov-like second-order central scheme was developed by Nessyahu and Tadmor (NT) in [38] (see also [45]). It was extended to higher-order of accuracy as well as for more space dimensions (consult [2], [19], [3] and [23], for the two-dimensional case, and [44], [17], [34] for the third-order schemes).

The NT scheme is based on reconstructing, in each time step, a piecewise-polynomial interpolant from the cell-averages computed in the previous time step. This interpolant is then (exactly) evolved in time, and finally, it is projected on its staggered averages, resulting with the staggered cell-averages at the next time-step. The one- and two-dimensional second-order schemes, are based on a piecewise-linear MUSCL-type reconstruction, whereas the third-order schemes are based on the non-oscillatory piecewise-parabolic reconstruction [33], [34]. Higher orders schemes are treated in [7], [28], [29]. Schemes base on staggered stencils, such as the NT scheme, are necessarily *redundant*. The use of redundant stencils was

extended to multi-dimensional *overlapping cells*, and as an example, we mention in this context the recent works on central discontinuous Galerkin methods, [35], [36], [37].

Like *upwind* schemes, the reconstructed piecewise-polynomials used by the central schemes, also make use of non-linear limiters which guarantee the overall non-oscillatory nature of the approximate solution. But unlike the upwind schemes, central schemes avoid the intricate and time consuming Riemann solvers; this advantage is particularly important in the multi-dimensional setup, where no such Riemann solvers are available.

**2. A short guide to Godunov-type schemes.** We want to solve the hyperbolic system of conservation laws

$$u_t + f(u)_x = 0 \quad (2.1)$$

by Godunov-type schemes. To this end we proceed in two steps. First, we introduce a small spatial scale,  $\Delta x$ , and we consider the corresponding (Steklov) sliding average of  $u(\cdot, t)$ ,

$$\bar{u}(x, t) := \frac{1}{|I_x|} \int_{I_x} u(\xi, t) d\xi, \quad I_x = \left\{ \xi \mid |\xi - x| \leq \frac{\Delta x}{2} \right\}.$$

The sliding average of (2.1) then yields

$$\bar{u}_t(x, t) + \frac{1}{\Delta x} \left[ f(u(x + \frac{\Delta x}{2}, t)) - f(u(x - \frac{\Delta x}{2}, t)) \right] = 0. \quad (2.2)$$

Next, we introduce a small time-step,  $\Delta t$ , and integrate over the slab  $t \leq \tau \leq t + \Delta t$ ,

$$\begin{aligned} \bar{u}(x, t + \Delta t) &= \bar{u}(x, t) \\ &- \frac{1}{\Delta x} \left[ \int_{\tau=t}^{t+\Delta t} f(u(x + \frac{\Delta x}{2}, \tau)) d\tau - \int_{\tau=t}^{t+\Delta t} f(u(x - \frac{\Delta x}{2}, \tau)) d\tau \right]. \end{aligned} \quad (2.3)$$

We end up with an equivalent reformulation of the conservation law (2.1): it expresses the precise relation between the sliding averages,  $\bar{u}(\cdot, t)$ , and their underlying pointvalues,  $u(\cdot, t)$ . We shall use this reformulation, (2.3), as the starting point for the construction of Godunov-type schemes.

We construct an approximate solution,  $w(\cdot, t^n)$ , at the discrete time-levels,  $t^n = n\Delta t$ . Here,  $w(x, t^n)$  is a piecewise polynomial written in the form

$$w(x, t^n) = \sum p_j(x) \chi_j(x), \quad \chi_j(x) := 1_{I_j},$$

where  $p_j(x)$  are algebraic polynomials supported at the discrete cells,  $I_j = I_{x_j}$ , centered around the midpoints,  $x_j := j\Delta x$ . An *exact* evolution of  $w(\cdot, t^n)$  based on (2.3), reads

$$\begin{aligned} \bar{w}(x, t^{n+1}) &= \bar{w}(x, t^n) \\ &- \frac{1}{\Delta x} \left[ \int_{t^n}^{t^{n+1}} f(w(x + \frac{\Delta x}{2}, \tau)) d\tau - \int_{t^n}^{t^{n+1}} f(w(x - \frac{\Delta x}{2}, \tau)) d\tau \right]. \end{aligned} \quad (2.4)$$

To construct a Godunov-type scheme, we *realize* (2.4) — or at least an accurate approximation of it, at discrete gridpoints. Here, we distinguish between the main methods, according to their way of *sampling* (2.4): these two main sampling methods correspond to upwind schemes and central schemes.

**2.1. Upwind schemes.** Let  $\bar{w}_j^n$  abbreviates the cell averages,  $\bar{w}_j^n := \frac{1}{\Delta x} \int_{I_j} w(\xi, t^n) d\xi$ . By sampling (2.4) at the *mid-cells*,  $x = x_j$ , we obtain an evolution scheme for these averages, which reads

$$\bar{w}_j^{n+1} = \bar{w}_j^n - \frac{1}{\Delta x} \left[ \int_{\tau=t^n}^{t^{n+1}} f(w(x_{j+\frac{1}{2}}, \tau)) d\tau - \int_{\tau=t^n}^{t^{n+1}} f(w(x_{j-\frac{1}{2}}, \tau)) d\tau \right]. \quad (2.5)$$

Here, it remains to recover the *pointvalues*,  $\{w(x_{j+\frac{1}{2}}, \tau)\}_j$ ,  $t^n \leq \tau \leq t^{n+1}$ , in terms of their known cell averages,  $\{\bar{w}_j^n\}_j$ , and to this end we proceed in two steps:

- First, the *reconstruction* — we recover the pointwise values of  $w(\cdot, \tau)$  at  $\tau = t^n$ , by a reconstruction of a piecewise polynomial approximation

$$w(x, t^n) = \sum_j p_j(x) \chi_j(x), \quad \bar{p}_j(x_j) = \bar{w}_j^n. \quad (2.6)$$

- Second, the *evolution* —  $w(x_{j+\frac{1}{2}}, \tau \geq t^n)$  are determined as the solutions of the generalized Riemann problems

$$w_t + f(w)_x = 0, \quad t \geq t^n; \quad w(x, t^n) = \begin{cases} p_j(x) & x < x_{j+\frac{1}{2}}, \\ p_{j+1}(x) & x > x_{j+\frac{1}{2}}. \end{cases} \quad (2.7)$$

The solution of (2.7) is composed of a family of nonlinear waves — left-going and right-going waves. An exact Riemann solver, or at least an approximate one is used to distribute these nonlinear waves between the two neighboring cells,  $I_j$  and  $I_{j+1}$ . It is this distribution of waves according to their direction which is responsible for *upwind differencing*, consult Figure 2.1. We briefly recall few canonical examples for this category of upwind Godunov-type schemes.

The original Godunov scheme is based on piecewise-constant reconstruction,  $w(x, t^n) = \Sigma \bar{w}_j^n \chi_j$ , followed by an exact Riemann solver. This results in a first-order accurate upwind method [14], which is the forerunner for all other Godunov-type schemes. A second-order extension was introduced by van Leer [21]: his MUSCL scheme reconstructs a piecewise linear approximation,  $w(x, t^n) = \Sigma p_j(x) \chi_j(x)$ , with linear pieces of

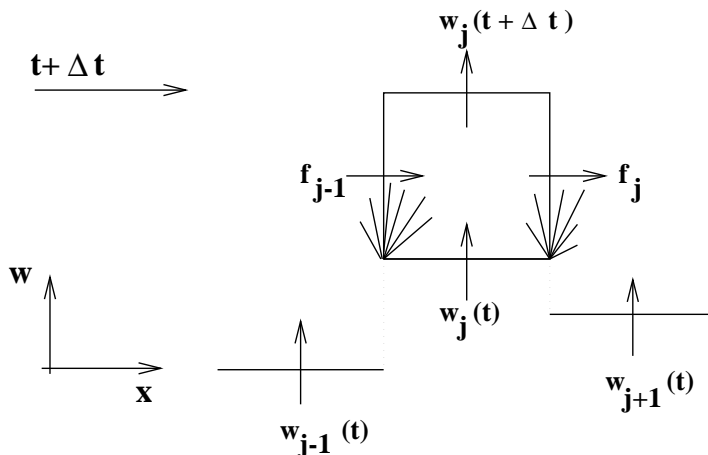


FIG. 1. Upwind differencing by Godunov-type scheme.

the form  $p_j(x) = \bar{w}_j^n + w'_j \left( \frac{x-x_j}{\Delta x} \right)$  so that  $\bar{p}_j(x_j) = \bar{w}_j^n$ . Here the  $w'_j$ -s are possibly limited slopes which are reconstructed from the known cell-averages,  $w'_j = \{(w_j^n)'\} = \{w'(\bar{w}_k^n)_{k=j-1}^{j+1}\}$ . (Throughout this lecture we use primes,  $w'_j, w''_j, \dots$ , to denote *discrete* derivatives, which approximate the corresponding differential ones). A whole library of limiters is available in this context, so that the co-monotonicity of  $w(x, t^n)$  with  $\Sigma \bar{w}_j \chi_j$  is guaranteed, e.g., [46]. The Piecewise-Parabolic Method (PPM) of Colella-Woodward [9] and respectively, ENO schemes of Harten et.al. [16], offer, respectively, third- and higher-order Godunov-type upwind schemes. (A detailed account of ENO schemes can be found in lectures of C.W. Shu in this volume). Finally, we should not give the impression that limiters are used exclusively in conjunction with Godunov-type schemes. The *positive schemes* of Liu and Lax, [32], offer simple and fast upwind schemes for multidimensional systems, based on an alternative positivity principle.

**2.2. Central schemes.** As before, we seek a piecewise-polynomial,  $w(x, t^n) = \Sigma p_j(x) \chi_j(x)$ , which serves as an approximate solution to the *exact* evolution of sliding averages in (2.4),

$$\begin{aligned} \bar{w}(x, t^{n+1}) &= \bar{w}(x, t^n) \\ &- \frac{1}{\Delta x} \left[ \int_{t^n}^{t^{n+1}} f\left(w\left(x + \frac{\Delta x}{2}, \tau\right)\right) d\tau - \int_{t^n}^{t^{n+1}} f\left(w\left(x - \frac{\Delta x}{2}, \tau\right)\right) d\tau \right]. \end{aligned} \quad (2.8)$$

Note that the polynomial pieces of  $w(x, t^n)$  are supported in the cells,  $I_j = \left\{ \xi \mid \left| \xi - x_j \right| \leq \frac{\Delta x}{2} \right\}$ , with interfacing breakpoints at the half-integers gridpoints,  $x_{j+\frac{1}{2}} = \left( j + \frac{1}{2} \right) \Delta x$ .

We recall that upwind schemes (2.5) were based on sampling (2.4) in the *midcells*,  $x = x_j$ . In contrast, central schemes are based on sampling (2.8) at the *interfacing breakpoints*,  $x = x_{j+\frac{1}{2}}$ , which yields

$$\bar{w}_{j+\frac{1}{2}}^{n+1} = \bar{w}_{j+\frac{1}{2}}^n - \frac{1}{\Delta x} \left[ \int_{\tau=t^n}^{t^{n+1}} f(w(x_{j+1}, \tau)) d\tau - \int_{\tau=t^n}^{t^{n+1}} f(w(x_j, \tau)) d\tau \right]. \quad (2.9)$$

We want to utilize (2.9) in terms of the known cell averages at time level  $\tau = t^n$ ,  $\{\bar{w}_j^n\}_j$ . The remaining task is therefore to recover the *pointvalues*  $\{w(\cdot, \tau) \mid t^n \leq \tau \leq t^{n+1}\}$ , and in particular, the *staggered averages*,  $\{\bar{w}_{j+\frac{1}{2}}^n\}$ . As before, this task is accomplished in two main steps:

- First, we use the given cell averages  $\{\bar{w}_j^n\}_j$ , to *reconstruct* the pointvalues of  $w(\cdot, \tau = t^n)$  as piecewise polynomial approximation

$$w(x, t^n) = \sum_j p_j(x) \chi_j(x), \quad \bar{p}_j(x_j) = \bar{w}_j^n. \quad (2.10)$$

In particular, the staggered averages on the right of (2.9) are given by

$$\bar{w}_{j+\frac{1}{2}}^n = \frac{1}{\Delta x} \left[ \int_{x_j}^{x_{j+\frac{1}{2}}} p_j(x) dx + \int_{x_{j+\frac{1}{2}}}^{x_{j+1}} p_{j+1}(x) dx \right]. \quad (2.11)$$

The resulting central scheme (2.9) then reads

$$\begin{aligned} \bar{w}_{j+\frac{1}{2}}^{n+1} &= \frac{1}{\Delta x} \left[ \int_{x_j}^{x_{j+\frac{1}{2}}} p_j(x) dx + \int_{x_{j+\frac{1}{2}}}^{x_{j+1}} p_{j+1}(x) dx \right] + \\ &- \frac{1}{\Delta x} \left[ \int_{\tau=t^n}^{t^{n+1}} f(w(x_{j+1}, \tau)) d\tau - \int_{\tau=t^n}^{t^{n+1}} f(w(x_j, \tau)) d\tau \right]. \end{aligned} \quad (2.12)$$

- Second, we follow the *evolution* of the pointvalues along the mid-cells,  $x = x_j$ ,  $\{w(x_j, \tau \geq t^n)\}_j$ , which are governed by

$$w_t + f(w)_x = 0, \quad \tau \geq t^n; \quad w(x, t^n) = p_j(x) \quad x \in I_j. \quad (2.13)$$

Let  $\{a_k(u)\}_k$  denote the eigenvalues of the Jacobian  $A(u) := \frac{\partial f}{\partial u}$ . By hyperbolicity, information regarding the interfacing discontinuities at  $(x_{j\pm\frac{1}{2}}, t^n)$  propagates no faster than  $\max_k |a_k(u)|$ . Hence, the mid-cells values governed by (2.13),  $\{w(x_j, \tau \geq t^n)\}_j$ , remain free of discontinuities, at least for sufficiently small time step dictated by the CFL condition  $\Delta t \leq \frac{1}{2} \Delta x \cdot \max_k |a_k(u)|$ . Consequently, since the numerical fluxes on the right of (2.12),  $\int_{\tau=t^n}^{t^{n+1}} f(w(x_j, \tau)) d\tau$ , involve only smooth integrands, they can be computed within any degree of desired accuracy by an appropriate quadrature rule.

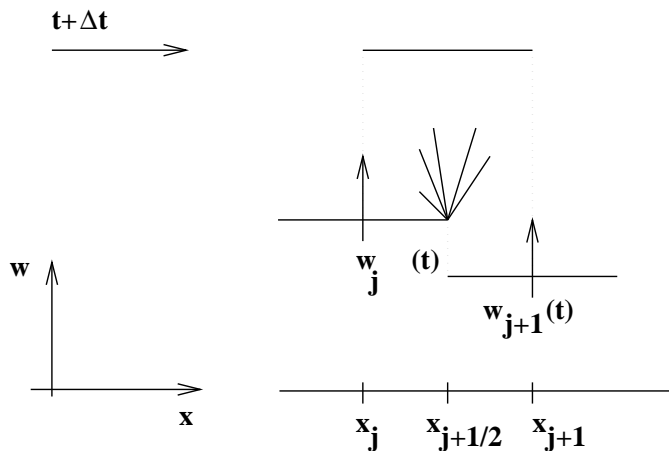


FIG. 2. Central differencing by Godunov-type scheme.

It is the *staggered* averaging over the fan of left-going and right-going waves centered at the half-integrated interfaces,  $(x_{j+\frac{1}{2}}, t^n)$ , which characterizes the *central* differencing, consult Figure 2.2. A main feature of these central schemes – in contrast to upwind ones, is the computation of *smooth* numerical fluxes along the mid-cells,  $(x = x_j, \tau \geq t^n)$ , which avoids the costly (approximate) Riemann solvers. A couple of examples of central Godunov-type schemes is in order.

The first-order Lax-Friedrichs (LxF) approximation is the forerunner for such central schemes — it is based on piecewise constant reconstruction,  $w(x, t^n) = \sum p_j(x) \chi_j(x)$  with  $p_j(x) = \bar{w}_j^n$ . The resulting central scheme, (2.12), then reads (with the usual fixed mesh ratio  $\lambda := \frac{\Delta t}{\Delta x}$ )

$$\bar{w}_{j+\frac{1}{2}}^{n+1} = \frac{1}{2}(\bar{w}_j^n + \bar{w}_{j+1}^n) - \lambda \left[ f(\bar{w}_{j+1}^n) - f(\bar{w}_j^n) \right]. \quad (2.14)$$

Our main focus in the rest of this chapter is on non-oscillatory higher-order extensions of the LxF schemes.

### 3. Central schemes in one-space dimension.

**3.1. The second-order Nessyahu-Tadmor scheme.** In this section we overview the construction of high-resolution central schemes in one-space dimension. We begin with the reconstruction of the second-order, non-oscillatory Nessyahu and Tadmor (NT) scheme, [38]. To approximate solutions of (2.1), we introduce a piecewise-linear approximate solution at the discrete time levels,  $t^n = n\Delta t$ , based on linear functions  $p_j(x, t^n)$  which are supported at the cells  $I_j$  (see Figure 3),

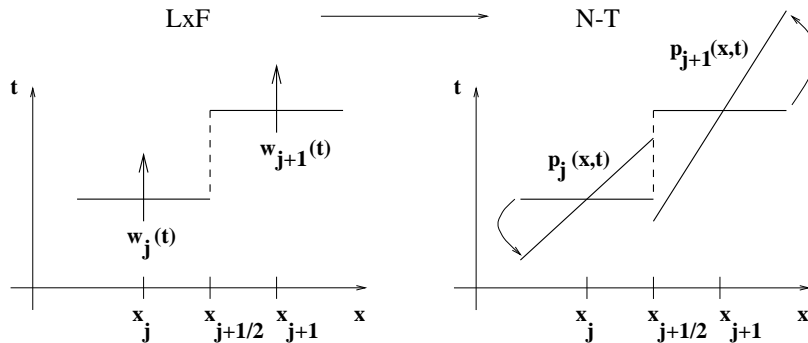


FIG. 3. The second-order reconstruction.

$$w(x, t)|_{t=t^n} = \sum_j p_j(x, t^n) \chi_j(x) := \sum_j \left[ \bar{w}_j^n + w'_j \left( \frac{x - x_j}{\Delta x} \right) \right] \chi_j(x),$$

$$\chi_j(x) := 1_{I_j}. \quad (3.1)$$

Second-order of accuracy is guaranteed if the discrete slopes approximate the corresponding derivatives,  $w'_j \sim \Delta x \cdot \partial_x w(x_j, t^n) + O(\Delta x)^2$ . At the same time, the second-order reconstruction is sought to be *non-oscillatory* in a manner which is properly quantified in terms of a maximum principle, total variation bound etc. To maintain both – second-order accuracy and the non-oscillatory character of the reconstruction, one may choose from a large class of *nonlinear limiters*, e.g., [21], [15], [46], [33]. We mention here the canonical class of limiters of the form

$$w'_j = MM\{\theta(\bar{w}_{j+1}^n - \bar{w}_j^n), \frac{1}{2}(\bar{w}_{j+1}^n - \bar{w}_{j-1}^n), \theta(\bar{w}_j^n - \bar{w}_{j-1}^n)\}. \quad (3.2)$$

Here and below,  $\theta \in [1, 2]$  is a free parameter which limits the maximal reconstructed slope, and  $MM$  denotes the so-called min-mod function

$$MM\{x_1, x_2, \dots\} = \begin{cases} \min_i \{x_i\} & \text{if } x_i > 0, \forall i \\ \max_i \{x_i\} & \text{if } x_i < 0, \forall i \\ 0 & \text{otherwise.} \end{cases}$$

An *exact* evolution of  $w$ , based on integration of the conservation law over the staggered cell,  $I_{j+\frac{1}{2}}$ , then reads, (2.9)

$$\bar{w}_{j+\frac{1}{2}}^{n+1} = \frac{1}{\Delta x} \int_{I_{j+\frac{1}{2}}} w(x, t^n) dx - \frac{1}{\Delta x} \int_{\tau=t^n}^{t^{n+1}} [f(w(x_{j+1}, \tau)) - f(w(x_j, \tau))] d\tau.$$

The first integral is the staggered cell-average at time  $t^n$ ,  $\bar{w}_{j+\frac{1}{2}}^n$ , which can be computed directly from the above reconstruction,

$$\bar{w}_{j+\frac{1}{2}}^n := \frac{1}{\Delta x} \int_{x_j}^{x_{j+1}} w(x, t^n) dx = \frac{1}{2}(\bar{w}_j^n + \bar{w}_{j+1}^n) + \frac{1}{8}(w'_j - w'_{j+1}). \quad (3.3)$$

The time integrals of the flux are computed by the second-order accurate mid-point quadrature rule

$$\int_{\tau=t^n}^{t^{n+1}} f(w(x_j, \tau)) d\tau \sim \Delta t \cdot f(w(x_j, t^{n+\frac{1}{2}})).$$

Here, the Taylor expansion is being used to predict the required mid-values of  $w$

$$\begin{aligned} w(x_j, t^{n+\frac{1}{2}}) &\sim w(x_j, t) + \frac{\Delta t}{2} w_t(x_j, t^n) \\ &= \bar{w}_j^n - \frac{\Delta t}{2} A(\bar{w}_j^n) (p_j(x_j, t^n))_x = \bar{w}_j^n - \frac{\lambda}{2} A_j^n w'_j. \end{aligned}$$

In summary, we end up with the central scheme, [38], which consists of a first-order *predictor step*,

$$w_j^{n+\frac{1}{2}} = \bar{w}_j^n - \frac{\lambda}{2} A_j^n w'_j, \quad A_j^n := A(\bar{w}_j^n), \quad (3.4)$$

followed by the second-order *corrector step*, (2.12),

$$\bar{w}_{j+\frac{1}{2}}^{n+1} = \frac{1}{2}(\bar{w}_j^n + \bar{w}_{j+1}^n) + \frac{1}{8}(w'_j - w'_{j+1}) - \lambda \left[ f(w_{j+1}^{n+\frac{1}{2}}) - f(w_j^{n+\frac{1}{2}}) \right]. \quad (3.5)$$

The *scalar* non-oscillatory properties of (3.4)–(3.5) were proved in [38], including the TVD property, cell entropy inequality,  $L_{loc}^1$  – error estimates, etc. Moreover, the numerical experiments, reported in [38], [3], [5], [43], [1], [7], with one-dimensional *systems* of conservation laws, show that such second-order central schemes enjoy the same high-resolution as the corresponding second-order upwind schemes do. The main difference lies in the resolution of linear contact waves, where upwind differencing in the *characteristic* eigen-directions yields improved resolution; but see [25], [31] for example of enhancing the resolution of contact discontinuities in central schemes. Thus, the excessive smearing typical to the first-order LxF central scheme is compensated here by the second-order accurate MUSCL reconstruction.

In Figure 4 we compare, side by side, the upwind ULT scheme of Harten, [15], with our central scheme (3.4)–(3.5). The comparable high-resolution of this so called Lax’s Riemann problem is evident.

At the same time, the central scheme (3.4)–(3.5) has the advantage over the corresponding upwind schemes, in that no (approximate) Riemann solvers, as in (2.7), are required. Hence, these Riemann-free central schemes provide an efficient high-resolution alternative in the one-dimensional case, and a particularly advantageous framework for multidimensional computations, e.g., [3], [19]. This advantage in the multidimensional case will be explored in the next section. Also, *staggered* central differencing, along the lines of the Riemann-free Nessyahu-Tadmor scheme (3.4)–(3.5), admits

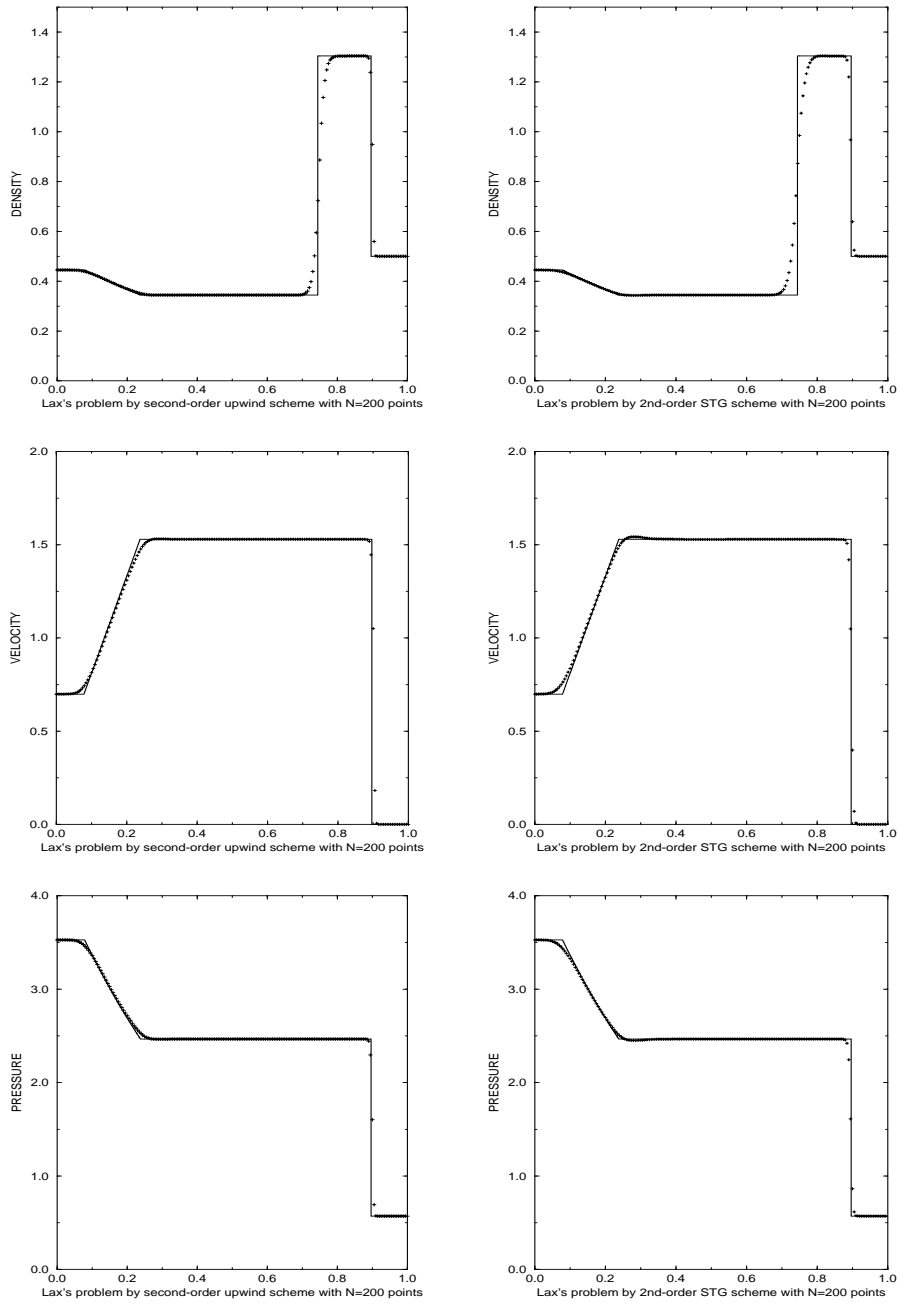


FIG. 4. 2nd order: central (STG) vs. upwind (ULT) — Lax's Riemann problem.

simple efficient extensions in the presence of general source terms, [11], [40] and in particular, stiff source terms. Indeed, it is a key ingredient behind the relaxation schemes studied in [20].

It should be noted, however, that the component-wise version of these central schemes might result in deterioration of resolution at the computed extrema. The second-order computation presented in Figure 5 below demonstrates this point. (this will be corrected by higher order central methods). Of course, this – so called extrema clipping, is typical to high-resolution upwind schemes as well; but it is more pronounced with our central schemes due to the built-in extrema-switching to the dissipative LxF scheme. Indeed, once an extrema cell,  $I_j$ , is detected (by the limiter), it sets a zero slope,  $w'_j = 0$ , in which case the second-order scheme (3.4)–(3.5) is reduced back to the first-order LxF, (2.14).

**3.2. The third-order central scheme.** Following the framework outlined in §3.1, the upgrade to third-order central scheme consists of two main ingredients:

- (i) A third-order accurate, piecewise-quadratic polynomial reconstruction which enjoys desirable non-oscillatory properties;
- (ii) An appropriate quadrature rule to approximate the numerical fluxes along cells' interfaces.

Following [34], we proceed as follows. The piecewise-parabolic reconstruction takes the form

$$p_j(x) = w_j^n + w'_j \left( \frac{x - x_j}{\Delta x} \right) + \frac{1}{2} w''_j \left( \frac{x - x_j}{\Delta x} \right)^2. \quad (3.6)$$

Here,  $w''_j$  are the (pointvalues of) the *reconstructed second derivatives*

$$w''_j := \theta_j \Delta_+ \Delta_- \bar{w}_j^n; \quad (3.7)$$

$w'_j$  are the (pointvalues of) the *reconstructed slopes*,

$$w'_j := \theta_j \Delta_0 \bar{w}_j^n; \quad (3.8)$$

and  $w_j^n$  are the *reconstructed pointvalues*

$$w_j^n := \bar{w}_j^n - \frac{w''_j}{24}. \quad (3.9)$$

Observe that, starting with third- (and higher-) order accurate methods, pointwise values *cannot* be interchanged with cell averages,  $w_j^n \neq \bar{w}_j^n$ .

Here,  $\theta_j$  are appropriate nonlinear limiters which guarantee the non-oscillatory behavior of the third-order reconstruction; its precise form can be found in [33], [34]. They guarantee that the reconstruction (3.6) is non-oscillatory in the sense that  $N(w(\cdot, t^n))$  — the number of extrema

of  $w(x, t^n)$ , does not exceed that of its piecewise-constant projection,  $N(\Sigma \bar{w}_j^n \chi_j(\cdot))$ ,

$$N(w(\cdot, t^n)) \leq N(\Sigma \bar{w}_j^n \chi_j(\cdot)). \quad (3.10)$$

Next we turn to the evolution of the piecewise-parabolic reconstructed solution. To this end we need to evaluate the staggered averages,  $\{\bar{w}_{j+\frac{1}{2}}^n\}$ , and to approximate the interface fluxes,  $\left\{ \int_{\tau=t^n}^{t^{n+1}} f(w(x_j, \tau)) d\tau \right\}$ .

With  $p_j(x) = w_j^n + w_j' \left( \frac{x-x_j}{\Delta x} \right) + \frac{1}{2} w_j'' \left( \frac{x-x_j}{\Delta x} \right)^2$  specified in (3.6)–(3.9), one evaluates the staggered averages of the third order reconstruction  $w(x, t^n) = \Sigma p_j(x) \chi_j(x)$

$$\bar{w}_{j+\frac{1}{2}}^n = \frac{1}{\Delta x} \int_{x_j}^{x_{j+1}} w(x, t^n) dx = \frac{1}{2} (\bar{w}_j + \bar{w}_{j+1}) + \frac{1}{8} (w_j' - w_{j+1}'). \quad (3.11)$$

Remarkably, we obtain here the same formula for the staggered averages as in the second-order cases, consult (3.3); the only difference is the use of the new limited slopes in (3.8),  $w_j' = \theta_j \Delta_0 \bar{w}_j^n$ .

Next, we approximate the (exact) numerical fluxes by Simpson's quadrature rule, which is (more than) sufficient for retaining the overall third-order accuracy,

$$\frac{1}{\Delta x} \int_{\tau=t^n}^{t^{n+1}} f(w(x_j, \tau)) d\tau \sim \frac{\lambda}{6} \left[ f(w_j^n) + 4f(w_j^{n+\frac{1}{2}}) + f(w_j^{n+1}) \right]. \quad (3.12)$$

This in turn, requires the three approximate *pointvalues* on the right,  $w_j^{n+\beta} \sim w(x_j, t^{n+\beta})$  for  $\beta = 0, \frac{1}{2}, 1$ . Following our approach in the second-order case, [38], we use Taylor expansion to *predict*

$$w_j^n = \bar{w}_j^n - \frac{w_j''}{24}; \quad (3.13)$$

$$\begin{aligned} \dot{w}_j^n &\equiv (\Delta x \cdot \partial_t) w(x_j, t^n) = -\Delta x \cdot \partial_x f(w(x_j, t^n)) \\ &= -a(w_j^n) \cdot w_j', ; \end{aligned} \quad (3.14)$$

$$\begin{aligned} \ddot{w}_j^n &\equiv (\Delta x \cdot \partial_t)^2 w(x_j, t^n) = \Delta x \cdot \partial_x \left[ a(w_j^n) \Delta x \cdot \partial_x f(w(x_j, t^n)) \right] \\ &= a^2(w_j^n) w_j'' + 2a(w_j^n) a'(w_j^n) (w_j')^2. \end{aligned} \quad (3.15)$$

In summary of the scalar setup, we end up with a two step scheme where, starting with the reconstructed pointvalues

$$w_j^n = \bar{w}_j^n - \frac{w_j''}{24}, \quad (3.16)$$

we *predict* the pointvalues  $w_j^{n+\beta}$  by, e.g. Taylor expansions,

$$w_j^{n+\beta} = w_j^n + \lambda\beta\dot{w}_j^n + \frac{(\lambda\beta)^2}{2}\ddot{w}_j^n, \quad \beta = \frac{1}{2}, 1; \quad (3.17)$$

this is followed by the *corrector* step

$$\begin{aligned} \bar{w}_{j+\frac{1}{2}}^n &= \frac{1}{2}(\bar{w}_j^n + \bar{w}_{j+1}^n) + \frac{1}{8}(w'_j - w'_{j+1}) \\ &\quad - \frac{\lambda}{6} \left\{ \left[ f(w_{j+1}^n) + 4f(w_{j+1}^{n+\frac{1}{2}}) + f(w_{j+1}^{n+1}) \right] \right. \\ &\quad \left. - \left[ f(w_j^n) + 4f(w_j^{n+\frac{1}{2}}) + f(w_j^{n+1}) \right] \right\}. \end{aligned} \quad (3.18)$$

In Figure 5 we revisit the so called Woodward-Colella problem, [49], where we compare the second vs. the third-order results. The improvement in resolving the density field is evident.

We conclude this section with several remarks.

REMARK.

1. Stability.

We briefly mention the stability results for the scalar central schemes. In the second order case, the NT scheme was shown to be both TVD and entropy stable in the sense of satisfying a cell entropy inequality – consult [38]. The third-order scalar central scheme is stable in the sense of satisfying the NED property, (3.10), namely

**THEOREM 3.1** ([34]). *Consider the central scheme (3.16), (3.17), (3.18), based on the third-order accurate quadratic reconstruction, (3.6)–(3.9). Then it satisfies the so-called Number of Extrema Diminishing (NED) property, in the sense that*

$$N \left( \sum_{\nu} \bar{w}_{v+\frac{1}{2}}^{n+1} \chi_{v+\frac{1}{2}}(x) \right) \leq N \left( \sum_{\nu} \bar{w}_{\nu}^n \chi_{\nu}(x) \right). \quad (3.19)$$

2. Source terms, radial coordinates, ...

Extensions of the central framework which deal with both, stiff and non-stiff source terms can be found in [43], [1], [11], [6]. In particular, Kupferman in [22], [23] developed the central framework within the radial coordinates which require to handle both – variable coefficients + source terms.

3. Higher order central schemes.

We refer to [7], where a high-order ENO reconstruction is realized by a staggered cell averaging. Here, intricate Riemann solvers are replaced by high order quadrature rules. and for this purpose, one can effectively use the RK method (rather than the Taylor expansion outlined above):

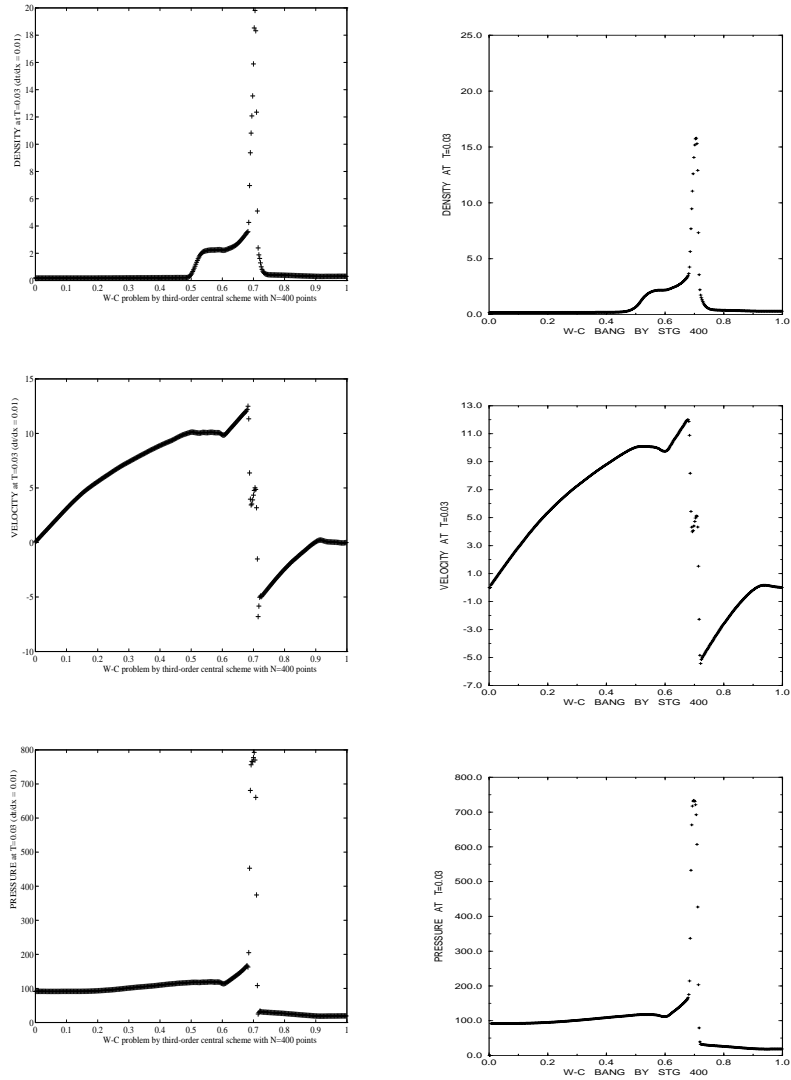


FIG. 5. 3<sup>rd</sup> vs. 2<sup>nd</sup> order central schemes — Woodward-Colella problem at  $t = 0.03$ .

#### 4. Taylor vs. Runge-Kutta.

The evaluations of Taylor expansions could be substituted by the more economical Runge-Kutta integrations; the simplicity becomes more pronounced with *systems*. A particular useful approach in this context was proposed in [7], [28], [29] using the natural continuous extensions of RK schemes.

## 5. Systems.

One of the main advantages of our central-staggered framework over that of the upwind schemes, is that expensive and time-consuming characteristic decompositions can be avoided. Specifically, all the non-oscillatory computations can be carried out with diagonal limiters, based on a *component-wise* extension of the scalar limiters outlined above.

**4. Central schemes in two space dimensions.** Following the one dimensional setup, one can derive a non-oscillatory, two-dimensional central scheme. Here we sketch the construction of the second-order two-dimensional scheme following [19] (see also [2]). For the two-dimensional third-order accurate scheme, we refer to [28].

We consider the two-dimensional hyperbolic system of conservation laws

$$u_t + f(u)_x + g(u)_y = 0. \quad (4.1)$$

To approximate a solution to (4.1), we start with a two-dimensional linear reconstruction

$$w(x, y, t^n) = \sum_{j,k} p_{j,k}(x, y) \chi_{j,k}(x, y), \quad (4.2)$$

$$p_{j,k}(x, y) = \bar{w}_{j,k}^n + w'_{j,k} \left( \frac{x - x_j}{\Delta x} \right) + w^{\flat}_{j,k} \left( \frac{y - y_k}{\Delta y} \right).$$

Here, the discrete slopes in the  $x$  and in the  $y$  direction approximate the corresponding derivatives,  $w'_{j,k} \sim \Delta x \cdot w_x(x_j, y_k, t^n) + O(\Delta x)^2$ ,  $w^{\flat}_{j,k} \sim \Delta y \cdot w_y(x_j, y_k, t^n) + O(\Delta y)^2$ , and  $\chi_{j,k}(x, y)$  is the characteristic function of the cell  $\mathcal{C}_{j,k} := \left\{ (\xi, \eta) \mid |\xi - x_j| \leq \frac{\Delta x}{2}, |\eta - y_k| \leq \frac{\Delta y}{2} \right\} = I_j \otimes J_k$ . Of course, it is essential to reconstruct the discrete slopes,  $w'$  and  $w^{\flat}$ , with *limiters*, which guarantee the non-oscillatory character of the reconstruction; the family of min-mod limiters is a prototype example

$$w'_{jk} = MM\left\{ \theta(\bar{w}_{j+1,k}^n - \bar{w}_{j,k}^n), \frac{1}{2}(\bar{w}_{j+1,k}^n - \bar{w}_{j-1,k}^n), \theta(\bar{w}_{j,k}^n - \bar{w}_{j-1,k}^n) \right\}, \quad (4.3')$$

$$1 \leq \theta \leq 2,$$

$$w^{\flat}_{jk} = MM\left\{ \theta(\bar{w}_{j,k+1}^n - \bar{w}_{j,k}^n), \frac{1}{2}(\bar{w}_{j,k+1}^n - \bar{w}_{j,k-1}^n), \theta(\bar{w}_{j,k}^n - \bar{w}_{j,k-1}^n) \right\}, \quad (4.3'')$$

$$1 \leq \theta \leq 2.$$

An exact evolution of this reconstruction, which is based on integration of the conservation law over the staggered volume yields

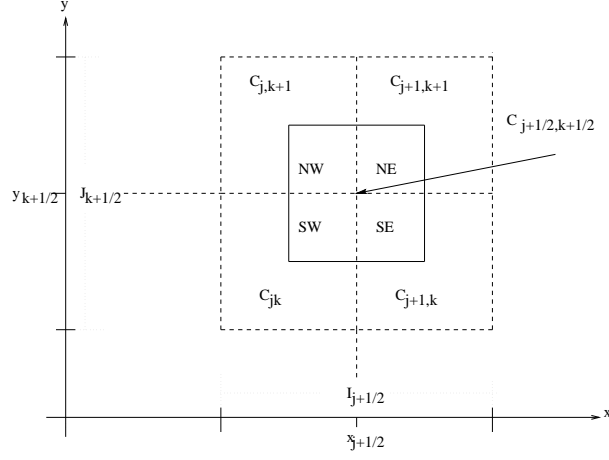


FIG. 6. Floor plan of the staggered grid.

$$\begin{aligned}
\bar{w}_{j+\frac{1}{2},k+\frac{1}{2}}^{n+1} &= \mathcal{f}_{C_{j+\frac{1}{2},k+\frac{1}{2}}} w(x, y, t^n) dx dy & (4.4) \\
&- \lambda \left\{ \mathcal{f}_{\tau=t^n}^{t^{n+1}} \mathcal{f}_{y \in J_{k+\frac{1}{2}}} [f(w(x_{j+1}, y, \tau)) - f(w(x_j, y, \tau))] dy d\tau \right\} \\
&- \mu \left\{ \mathcal{f}_{\tau=t^n}^{t^{n+1}} \mathcal{f}_{x \in I_{j+\frac{1}{2}}} [g(w(x, y_{k+1}, \tau)) - g(w(x, y_k, \tau))] dx d\tau \right\}.
\end{aligned}$$

Here and below,  $\mathcal{f}$  denotes the normalized integral,  $\mathcal{f}_{\Omega} := \frac{1}{|\Omega|} \int_{\Omega}$ .

The exact averages at  $t^n$  – consult the floor plan in Figure 6 yields

$$\begin{aligned}
\bar{w}_{j+\frac{1}{2},k+\frac{1}{2}}^n &:= \mathcal{f}_{C_{j+\frac{1}{2},k+\frac{1}{2}}} w(x, y, t^n) dx dy & (4.5) \\
&= \frac{1}{4} (\bar{w}_{jk}^n + \bar{w}_{j+1,k}^n + \bar{w}_{j,k+1}^n + \bar{w}_{j+1,k+1}^n) \\
&+ \frac{1}{16} \left\{ (w'_{jk} - w'_{j+1,k}) + (w'_{j,k+1} - w'_{j+1,k+1}) \right. \\
&\left. + (w''_{jk} - w''_{j,k+1}) + (w''_{j+1,k} - w''_{j+1,k+1}) \right\}.
\end{aligned}$$

So far everything is *exact*. We now turn to *approximate* the four fluxes on the right of (4.4), starting with the one along the East face,

consult Figure 7,  $\mathcal{f}_{t^n}^{t^{n+1}} \mathcal{f}_{J_{k+\frac{1}{2}}} f(w(x_{j+1}, y, \tau)) dy d\tau$ . We use the midpoint

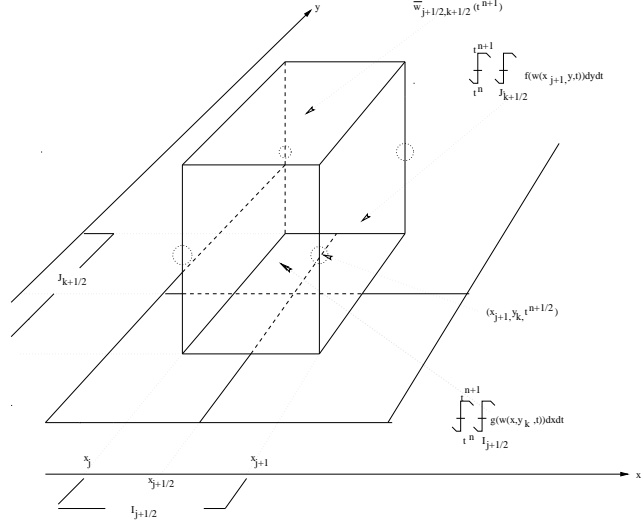


FIG. 7. The staggered stencil in two dimensions.

quadrature rule for second-order approximation of the temporal integral,  $\int_{y \in J_{k+\frac{1}{2}}} f(w(x_{j+1}, y, t^{n+\frac{1}{2}})) dy$ ; and, for reasons to be clarified below, we use the second-order rectangular quadrature rule for the spatial integration across the  $y$ -axis, yielding

$$\int_{t^n}^{t^{n+1}} \int_{y \in J_{k+\frac{1}{2}}} f(w(x_{j+1}, y, \tau)) dy d\tau \sim \frac{1}{2} \left[ f(w_{j+1,k}^{n+\frac{1}{2}}) + f(w_{j+1,k+1}^{n+\frac{1}{2}}) \right]. \quad (4.6)$$

In a similar manner we approximate the remaining fluxes.

These approximate fluxes make use of the midpoint values,  $w_{jk}^{n+\frac{1}{2}} \equiv w(x_j, y_k, t^{n+\frac{1}{2}})$ , and it is here that we take advantage of utilizing these midvalues for the spatial integration by the rectangular rule. Namely, since these midvalues are secured at the smooth center of their cells,  $C_{jk}$ , bounded away from the jump discontinuities along the edges, we may use Taylor expansion,  $w(x_j, y_k, t^{n+\frac{1}{2}}) = \bar{w}_{jk}^n + \frac{\Delta t}{2} w_t(x_j, y_k, t^n) + \mathcal{O}(\Delta t)^2$ . Finally, we use the conservation law (4.1) to express the time derivative,  $w_t$ , in terms of the spatial derivatives,  $f(w)'$  and  $g(w)'$ ,

$$w_{jk}^{n+\frac{1}{2}} = \bar{w}_{jk}^n - \frac{\lambda}{2} f(w)'_{jk} - \frac{\mu}{2} g(w)'_{jk}. \quad (4.7)$$

Here,  $f(w)'_{jk} \sim \Delta x \cdot f(w(x_j, y_k, t^n))_x$  and  $g(w)'_{jk} \sim \Delta y \cdot g(w(x_j, y_k, t^n))_y$ , are one-dimensional discrete slopes in the  $x$ - and  $y$ -directions, of the type reconstructed in (4.3')–(4.3''); for example, multiplication by the corresponding Jacobians  $A$  and  $B$  yields

$$f(w)'_{jk} = A(\bar{w}_{jk}^n)w'_{jk}, \quad g(w)\backslash_{jk} = B(\bar{w}_{jk}^n)w\backslash_{jk}.$$

Equipped with the midvalues (4.7), we can now evaluate the approximate fluxes, e.g., (4.6). Inserting these values, together with the staggered average computed in (4.6), into (4.4), we conclude with new staggered averages at  $t = t^{n+1}$ , given by

$$\begin{aligned} \bar{w}_{j+\frac{1}{2},k+\frac{1}{2}}^{n+1} &= \frac{1}{4}(\bar{w}_{jk}^n + \bar{w}_{j+1,k}^n + \bar{w}_{j,k+1}^n + \bar{w}_{j+1,k+1}^n) \\ &+ \frac{1}{16}(w'_{jk} - w'_{j+1,k}) - \frac{\lambda}{2} \left[ f(w_{j+1,k}^{n+\frac{1}{2}}) - f(w_{j,k}^{n+\frac{1}{2}}) \right] \\ &+ \frac{1}{16}(w'_{j,k+1} - w'_{j+1,k+1}) - \frac{\lambda}{2} \left[ f(w_{j+1,k+1}^{n+\frac{1}{2}}) - f(w_{j,k+1}^{n+\frac{1}{2}}) \right] \\ &+ \frac{1}{16}(w\backslash_{jk} - w\backslash_{j,k+1}) - \frac{\mu}{2} \left[ g(w_{j,k+1}^{n+\frac{1}{2}}) - g(w_{j,k}^{n+\frac{1}{2}}) \right] \\ &+ \frac{1}{16}(w\backslash_{j+1,k} - w\backslash_{j+1,k+1}) - \frac{\mu}{2} \left[ g(w_{j+1,k+1}^{n+\frac{1}{2}}) - g(w_{j+1,k}^{n+\frac{1}{2}}) \right]. \end{aligned} \quad (4.8)$$

In summary, we end up with a simple two-step predictor-corrector scheme which could be conveniently expressed in terms on the one-dimensional staggered averaging notations

$$\langle w_{j,\cdot} \rangle_{k+\frac{1}{2}} := \frac{1}{2}(w_{j,k} + w_{j,k+1}), \quad \langle w_{\cdot,k} \rangle_{j+\frac{1}{2}} := \frac{1}{2}(w_{j,k} + w_{j+1,k}).$$

Our scheme consists of a *predictor step*

$$w_{j,k}^{n+\frac{1}{2}} = w_{j,k}^n - \frac{\lambda}{2}f'_{j,k} - \frac{\mu}{2}g\backslash_{j,k}, \quad (4.9)$$

followed by the *corrector step*

$$\begin{aligned} \bar{w}_{j+\frac{1}{2},k+\frac{1}{2}}^{n+1} &= \langle \frac{1}{4}(\bar{w}_{j,\cdot}^n + \bar{w}_{j+1,\cdot}^n) + \frac{1}{8}(w'_{j,\cdot} - w'_{j+1,\cdot}) - \lambda(f_{j+1,\cdot}^{n+\frac{1}{2}} - f_{j,\cdot}^{n+\frac{1}{2}}) \rangle_{k+\frac{1}{2}} \\ &+ \langle \frac{1}{4}(\bar{w}_{\cdot,k}^n + \bar{w}_{\cdot,k+1}^n) + \frac{1}{8}(w\backslash_{\cdot,k} - w\backslash_{\cdot,k+1}) - \mu(g_{\cdot,k+1}^{n+\frac{1}{2}} - g_{\cdot,k}^{n+\frac{1}{2}}) \rangle_{j+\frac{1}{2}}. \end{aligned}$$

In Figures 8 taken from [19], we present the two-dimensional computation of a double-Mach reflection problem; in Figure 9 we quote from [5] the two-dimensional computation of MHD solution of Kelvin-Helmholtz instability due to shear flow. The computations are based on our second-order central scheme. It is remarkable that such a simple 'two-lines' algorithm, with no characteristic decompositions and no dimensional splitting, approximates the rather complicated double Mach reflection problem with such high resolution. Couple of remarks are in order.

- Two-dimensional computations using central schemes are sensitive to the choice of limiter being used. In the context of the double Mach reflection problem, for example, the  $MM_2$  (consult (3.2) with  $\theta = 2$ ) seems to yield the sharper results. the one-dimensional central scheme can be as sensitive as the 2D schemes.

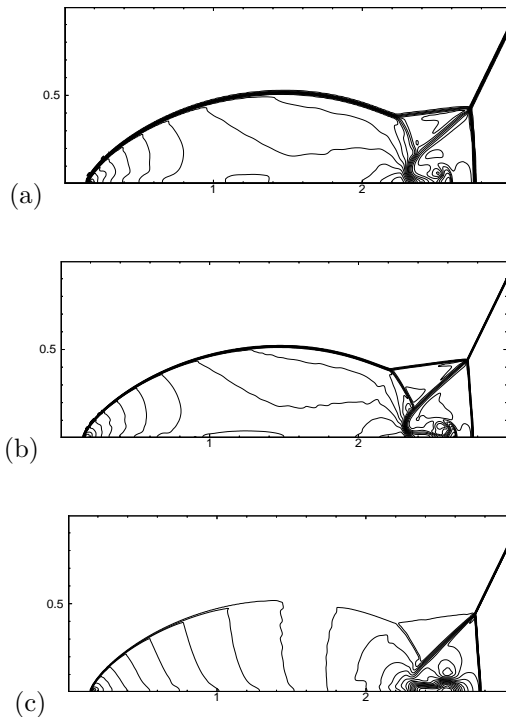


FIG. 8. *Double Mach reflection problem computed with the central scheme using  $MM_2$  limiter with  $CFL=0.475$  at  $t = 0.2$  (a) density computed with  $480 \times 120$  cells (b) density computed with  $960 \times 240$  cells (c)  $x$ -velocity computed with  $960 \times 240$  cells.*

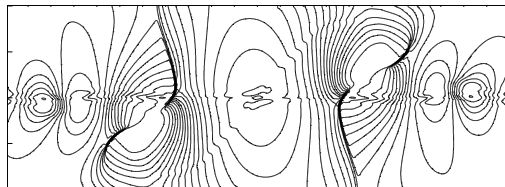


FIG. 9. *Kelvin-Helmholtz instability due to shear flow. Transverse configuration ( $B$  perpendicular to  $v$ ). Pressure contours at  $t = 140$ .*

- No effort was made to optimize the boundary treatment. The staggered stencils require a different treatment for even-odd cells intersecting with the boundaries. The lack of boundary resolution could be observed at the bottom of the two Mach stems.

We conclude this section with brief remarks on further results related to central schemes.

REMARK.

1. Simplicity.

Again, we would like to highlight the simplicity of the central schemes, which is particularly evident in the multidimensional setup: no characteristic information is required – in fact, even the exact Jacobians of the fluxes are not required; also, since no (approximate) Riemann solvers are involved, the central schemes require no dimensional splitting; as an example we refer to the approximation of the incompressible equations by central schemes, [24, 30]; the results in [10] provide another example of a *weakly* hyperbolic multidimensional system which could be efficiently solved in term of central schemes, by avoiding dimensional splitting.

2. Non-staggering. We refer to [18] for a non-staggered version of the central schemes.

3. Stability.

The following maximum principle holds for the nonoscillatory scalar central schemes:

THEOREM 4.1 ([19]). *Consider the two-dimensional scalar scheme (4.7–4.8), with minmod slopes,  $w'$  and  $w''$ , in (4.3'–4.3''). Then for any  $\theta < 2$  there exists a sufficiently small CFL number,  $C_\theta$  (– e.g.  $C_1 = (\sqrt{7} - 2)/6 \sim 0.1$ ), such that if the CFL condition is fulfilled,*

$$\max(\lambda \cdot \max_u |f_u(u)|, \mu \cdot \max_u |g_u(u)|) \leq C_\theta,$$

then the following local maximum principle holds

$$\min_{\substack{|p-(j+\frac{1}{2})|=\frac{1}{2} \\ |q-(k+\frac{1}{2})|=\frac{1}{2}}} \{\bar{w}_{p,q}^n\} \leq \bar{w}_{j+\frac{1}{2},k+\frac{1}{2}}^{n+1} \leq \max_{\substack{|p-(j+\frac{1}{2})|=\frac{1}{2} \\ |q-(k+\frac{1}{2})|=\frac{1}{2}}} \{\bar{w}_{p,q}^n\}. \quad (4.10)$$

## REFERENCES

- [1] A.M. ANILE, V. ROMANO, AND G. RUSSO, *Extended hydrodynamical model of carrier transport in semiconductors*, SIAM Journal Applied Mathematics, **61**, 2000, 74–101.
- [2] P. ARMINJON, D. STANESCU, AND M.-C. VIALON, *A Two-Dimensional Finite Volume Extension of the Lax-Friedrichs and Nessyahu-Tadmor Schemes for Compressible Flow*, Proc. of the 6th Internat. Symp. on Comp. Fluid Dynamics, (M. Hafez, K. Oshima eds.), Lake Tahoe, Nevada, September 1995, Vol. **IV**, pp. 7–14.
- [3] P. ARMINJON AND M.-C. VIALON, *Généralisation du Schéma de Nessyahu-Tadmor pour Une Équation Hyperbolique à Deux Dimensions D'espace*, C.R. Acad. Sci. Paris, **t. 320**, série I. (1995), pp. 85–88.
- [4] J. BALBAS AND E. TADMOR, CentPack: A package of high-resolution central schemes for nonlinear conservation laws and related problems, <http://www.cscamm.umd.edu/centpack/>.

- [5] J. BALBAS, E. TADMOR, AND C.-C. WU Non-oscillatory central schemes for one- and two-dimensional MHD equations *Journal of Computational Physics*, **201**, 2004, 261–285.
- [6] F. BEREUX AND L. SAINSAULIEU, *A Roe-type Riemann Solver for Hyperbolic Systems with Relaxation Based on Time-Dependent Wave Decomposition*, *Numer. Math.*, **77**, 1997, 143–185.
- [7] F. BIANCO, G. PUPPO, AND G. RUSSO, *High order central schemes for hyperbolic systems of conservation laws*, *SIAM J. Sci. Comp.*, **21**, 1999, 294–322.
- [8] D. L. BROWN, AND M. L. MINION *Performance of under-resolved two-dimensional incompressible flow simulations*, *J. Comp. Phys.*, **122**, 1985, 165–183.
- [9] P. COLELLA AND P. WOODWARD, *The piecewise parabolic method (PPM) for gas-dynamical simulations*, *JCP*, **54**, 1984, 174–201.
- [10] B. ENGQUIST AND O. RUNBORG, *Multi-phase computations in geometrical optics*, *Journal of Computational and Applied Mathematics*, **74**, 1996, 175–192.
- [11] ERBES, *A high-resolution Lax-Friedrichs scheme for Hyperbolic conservation laws with source term. Application to the Shallow Water equations*. Preprint.
- [12] K.O. FRIEDRICHS AND P.D. LAX, *Systems of Conservation Equations with a Convex Extension*, *Proc. Nat. Acad. Sci.*, **68**, 1971, 1686–1688.
- [13] E. GODLEWSKI, AND P.-A. RAVIART, *Hyperbolic Systems of Conservation Laws*, *Mathematics & Applications*, Ellipses, Paris, 1991.
- [14] S.K. GODUNOV, *A finite difference method for the numerical computation of discontinuous solutions of the equations of fluid dynamics*, *Mat. Sb.*, **47**, 1959, 271–290.
- [15] A. HARTEN, *High Resolution Schemes for Hyperbolic Conservation Laws*, *JCP*, **49**, 1983, 357–393.
- [16] A. HARTEN, B. ENGQUIST, S. OSHER, AND S.R. CHAKRAVARTHY, *Uniformly high order accurate essentially non-oscillatory schemes. III*, *JCP*, **71**, 1982, 231–303.
- [17] HUYNH, *A piecewise-parabolic dual-mesh method for the Euler equations*, AIAA-95-1739-CP, The 12th AIAA CFD Conf., 1995.
- [18] G.-S. JIANG, D. LEVY, C.-T. LIN, S. OSHER, AND E. TADMOR, *High-resolution Non-Oscillatory Central Schemes with Non-Staggered Grids for Hyperbolic Conservation Laws*, *SIAM Journal on Num. Anal.*, to appear.
- [19] G.-S JIANG AND E. TADMOR, *Nonoscillatory Central Schemes for Multidimensional Hyperbolic Conservation Laws*, *SIAM Journal on Scientific Computing*, **19**, 1998, 1892–1917.
- [20] S. JIN AND Z. XIN, *The relaxing schemes for systems of conservation laws in arbitrary space dimensions*, *Comm. Pure Appl. Math.*, **48**, 1995, 235–277.
- [21] B. VAN LEER, *Towards the Ultimate Conservative Difference Scheme, V. A Second-Order Sequel to Godunov’s Method*, *JCP*, **32**, 1979, 101–136.
- [22] R. KUPFERMAN, *Simulation of viscoelastic fluids: Couette-Taylor flow*, *J. Comp. Phys.*, **147**, 1998, 22–59
- [23] R. KUPFERMAN, *A numerical study of the axisymmetric Couette-Taylor problem using a fast high-resolution second-order central scheme*, *SIAM. J. Sci. Comp.*, **20**, 1998, 858–877.
- [24] R. KUPFERMAN AND E. TADMOR, *A Fast High-Resolution Second-Order Central Scheme for Incompressible Flow s*, *Proc. Nat. Acad. Sci.*, **94**, 1997, 4848–4852.
- [25] A. KURGANOV AND G. PETROVA, *Central schemes and contact discontinuities* *Mathematical Modelling and Numerical Analysis*, **34**, 2000, 1259–1275.
- [26] A. KURGANOV AND A. POLIZZI, *Non-oscillatory central schemes for traffic flow models with Arrhenius look-ahead dynamics*, *Netowrks and Heterogeneous Media*, **4**(3), 2009, 431–452.
- [27] R.J. LEVEQUE, *Numerical Methods for Conservation Laws*, *Lectures in Mathematics*, Birkhauser Verlag, Basel, 1992.
- [28] D. LEVY, G. PUPPO, AND G. RUSSO, *A third order central WENO scheme for 2D conservation laws* *Applied Numerical Mathematics*, **33**, 2000, 415–421.

- [29] D. LEVY, G. PUPPO, AND G. RUSSO, *A fourth-order central WENO scheme for multi-dimensional hyperbolic systems of conservation laws*, SIAM Journal on Scientific Computing, **24**, 2002, 480–506.
- [30] D. LEVY AND E. TADMOR, *Non-oscillatory Central Schemes for the Incompressible 2-D Euler Equations*, Math. Res. Let., **4**, 1997, 321–340.
- [31] K.-A. LIE AND S. NOELLE, *On the artificial compression method for second-order nonoscillatory central difference schemes for systems of conservation laws*, SIAM Journal on Scientific Computation, **24**, 2003, 1157–1174.
- [32] X.-D. LIU AND P.D. LAX, *Positive Schemes for Solving Multi-dimensional Hyperbolic Systems of Conservation Laws*, J. Comp. Fluid Dynamics, **5**(2), 1996, 133–156.
- [33] X.-D. LIU AND S. OSHER, *Nonoscillatory High Order Accurate Self-Similar Maximum Principle Satisfying Shock Capturing Schemes I*, SINUM, **33**(2), 1996, 760–779.
- [34] X.-D. LIU AND E. TADMOR, *Third Order Nonoscillatory Central Scheme for Hyperbolic Conservation Laws*, Numerische Mathematik, **79**, 1998, 397–425.
- [35] Y.-J. LIU, C.-W. SHU, E. TADMOR, AND M. ZHANG, *Central discontinuous Galerkin methods on overlapping cells with a non-oscillatory hierarchical reconstruction*, SIAM Journal on Numerical Analysis, **45**(6), 2007, 2442–2467.
- [36] Y.-J. LIU, C.-W. SHU, E. TADMOR, AND M. ZHANG, *Non-oscillatory hierarchical reconstruction for central and finite volume schemes*, Communications in Mathematical Physics, **2**(5), 2007, 933–963.
- [37] Y.-J. LIU, C.-W. SHU, E. TADMOR, AND M. ZHANG, *L2-stability analysis of the central discontinuous Galerkin method*, Mathematical Modelling and Numerical Analysis, **42**, 2008, 593–607.
- [38] H. NESSYAHU AND E. TADMOR, *Non-oscillatory Central Differencing for Hyperbolic Conservation Laws*, JCP, **87**(2), 1990, 408–463.
- [39] S. OSHER AND E. TADMOR, *On the Convergence of Difference Approximations to Scalar Conservation Laws*, Math. Comp., **50**(181), 1988, 19–51.
- [40] L. PARESCHI AND G. RUSSO, *Implicit Explicit Runge Kutta Schemes and Applications to Hyperbolic Systems with Relaxation*, J. Sci. Computing, **25**(1), 2005, 129–155.
- [41] P.L. ROE, *Approximate Riemann Solvers, Parameter Vectors, and Difference Schemes*, JCP, **43**, 1981, 357–372.
- [42] A. ROGERSON AND E. MEIBURG, *A numerical study of the convergence properties of ENO schemes*, J. Sci. Comput., **5**, 1990, 127–149.
- [43] V. ROMANO AND G. RUSSO, *Numerical solution for hydrodynamical models of semiconductors*, Mathematical Models and Applications in Applied Sciences, **10**(7), 2000, 1099–1120.
- [44] R. SANDERS, *A Third-order Accurate Variation Nonexpansive Difference Scheme for Single Conservation Laws*, Math. Comp., **41**, 1988, 535–558.
- [45] R. SANDERS AND A. WEISER, *A High Resolution Staggered Mesh Approach for Nonlinear Hyperbolic Systems of Conservation Laws*, JCP, **1010**, 1992, 314–329.
- [46] P.K. SWEBY, *High Resolution Schemes Using Flux Limiters for Hyperbolic Conservation Laws*, SINUM, **21**(5), 1984, 995–1011.
- [47] C.-W. SHU, *Numerical experiments on the accuracy of ENO and modified ENO schemes*, JCP, **5**, 1990, 127–149.
- [48] G. SOD, *A survey of several finite difference methods for systems of nonlinear hyperbolic conservation laws*, JCP, **22**, 1978, 1–31.
- [49] P. WOODWARD AND P. COLELLA, *The numerical simulation of two-dimensional fluid flow with strong shocks*, JCP, **54**, 1988, 115–173.